University Library

MINERVA ACCESS

A gateway to Melbourne's research publications

Minerva Access is the Institutional Repository of The University of Melbourne

Author/s:
Ge, C;Monk, IR;Monard, SC;Bedford, JG;Braverman, J;Stinear, TP;Wakim, LM

Title:
Neutrophils play an ongoing role in preventing bacterial pneumonia by blocking the dissemination of Staphylococcus aureus from the upper to the lower airways

Date:
2020-08-01

Citation:
Ge, C., Monk, I. R., Monard, S. C., Bedford, J. G., Braverman, J., Stinear, T. P. & Wakim, L. M. (2020). Neutrophils play an ongoing role in preventing bacterial pneumonia by blocking the dissemination of Staphylococcus aureus from the upper to the lower airways. Immunology and Cell Biology, 98 (7), pp.577-594. https://doi.org/10.1111/imcb.12343.

Persistent Link:
https://hdl.handle.net/11343/275874

Check for updates

MR JAMES G BEDFORD (Orcid ID : 0000-0001-5216-1779)

Article type : Original Article

# Neutrophils play an ongoing role in preventing bacterial pneumonia by blocking the dissemination of *S. aureus* from the upper to the lower airways.

Chenghao Ge[1,2*], Ian R. Monk[1*], Sarah C. Monard[1], James G. Bedford[1], Jessica Braverman[1], Timothy P. Stinear[1], and Linda M. Wakim[1]

[1]Department of Microbiology and Immunology, The University of Melbourne, at the Peter Doherty Institute for Infection and Immunity, Melbourne, Victoria 3000, Australia.

[2]School of Medicine, Tsinghua University, Beijing, China.

The authors have declared that no conflict of interest exists

*these authors contributed equally

**Key words**: *S. aureus*, neutrophils, bacterial pneumonia

**Running title.** Neutrophils confine *S. aureus* to the upper airways

**Correspondence**: LM Wakim (wakiml@unimelb.edu.au)
Linda M Wakim
Department of Microbiology & Immunology, University of Melbourne
The Doherty Institute for Infection & Immunity
Level 8, 792 Elizabeth Street, Melbourne, 3000, VIC Australia
Tel: +61-3-9035-4141; email: wakiml@unimelb.edu.au

This is the author manuscript accepted for publication and has undergone full peer review but has not been through the copyediting, typesetting, pagination and proofreading process, which may lead to differences between this version and the Version of Record. Please cite this article as doi: 10.1111/IMCB.12343

This article is protected by copyright. All rights reserved

Author Manuscript

Author Manuscript

**ABSTRACT**

*Staphylococcus aureus* is found in the nasal cavity of up to 30% of the human population. Persistent nasal carriage of *S. aureus* is a risk factor for influenza virus induced secondary bacterial pneumonia. To date, there is limited understanding of the factors that cause *S. aureus* to shift from the upper to the lower respiratory tract and convert from a commensal organism to an invasive pathogen. Here we show that neutrophils actively prevent *S. aureus* dissemination. Establishment of a mouse model of localised *S. aureus* nasal carriage revealed variations in the longevity of persistence of *S. aureus* isolates. Improved persistence within this site was associated with reduced nasal inflammation, less neutrophil egress into the airways and reduced neutrophil-bacteria association. Neutrophil depletion of mice with localised *S. aureus* nasal carriage triggered the development of an invasive *S. aureus* infection. Moreover, utilizing a model of influenza induced staphylococcal pneumonia we showed that treatment with granulocyte-colony stimulating factor (G-CSF), a potent enhancer of neutrophil number and function, significantly reduced bacterial loads in the lung and improved disease outcomes. This data reveals that neutrophils play an important and active role in confining *S. aureus* to the upper respiratory tract and highlights the use of approaches that improve neutrophil function as effective strategies to attenuate morbidity associated with staphylococcal pneumonia.

This article is protected by copyright. All rights reserved

Author Manuscript

## INTRODUCTION

A ubiquitous member of the normal human microbiota, the Gram-positive bacterium *Staphylococcus aureus* persistently and asymptomatically colonises the nasal cavity of up to 30% of the human population [1,2,3]. Yet given the opportunity, *S. aureus* has the ability to cause a wide range of infections and syndromes, including skin and soft tissue infections, toxic shock syndrome, bacteraemia, sepsis, and pneumonia. The clinical management of these invasive staphylococcal infections is complicated by widespread antibiotic resistance present in this bacterium[4]. *S. aureus* is one of the most common causes of hospital acquired infections, and it is recognized as the second-leading cause of infections in intensive care units[5]. Colonized individuals have a 2-10 fold increased risk of developing a nosocomial infection, with 80% of *S. aureus* invasive infections being caused by the patient's own endogenous colonizing strain[6,7]. To date, there is limited understanding of the factors that cause *S. aureus* to shift from the anterior nares, which serves as the principal habitat for this bacterium, to other organs, and in doing so, convert from a commensal organism to a pathogenic threat.

Although nasal colonization is not a prerequisite for staphylococcal disease, it has been identified as a major risk factor[6,8]. Of the many invasive infections mediated by *S. aureus*, pneumonia is among the most prominent, accounting for an estimated 50,000 staphylococcal infections per year (USA)[7]. *S. aureus* is the causative agent of 20-40% of hospital-acquired and ventilator-acquired pneumonias[9,10] as well as 9% of community-acquired pneumonias[11]. A major cofactor that increases mortality following *S. aureus* pneumonia is preceding influenza-like illness[12]. Although most cases of influenza virus infection alone are not fatal, superinfection of the lungs with *S. aureus* significantly heightens disease severity. Co-infected individuals are more often admitted into intensive care units and have a mortality rate of ~50%[13]. Given the substantial morbidity and mortality associated with influenza induced secondary bacterial pneumonia, the identification of immune targets to reduce bacterial pathogenesis will likely have major clinical benefits.

This article is protected by copyright. All rights reserved

Neutrophils are an essential component of the innate anti-bacterial immune response. They assist in bacterial eradication via many mechanisms, including phagocytic killing, the production of extracellular traps (NETs), the production of reactive oxygen species (ROS) and through the secretion of inflammatory cytokines[14, 15]. Neutrophils can respond to invasive *S. aureus* infection, rapidly being recruited to the nidus of infection and assisting in the eradication of the bacteria[16]. Here we investigated whether these cells also have a prophylactic role in blocking the transition of *S. aureus* from commensal organism to invasive pathogen. We show that neutrophils actively prevent the dissemination of *S. aureus* from the upper to the lower respiratory tract. Using a mouse model of localised *S. aureus* nasal carriage, we show that improved persistence of *S. aureus* isolates in the murine nares corelated with low level nasal inflammation, less neutrophil egress and reduced neutrophil-bacteria association in the airways. The depletion of neutrophils from mice with localised *S. aureus* nasal carriage resulted in dissemination of *S. aureus* from the nasal tissue into the inner ear and lung. Moreover, utilizing a model of influenza induced staphylococcal pneumonia we show that boosting neutrophil function as a result of granulocyte-colony stimulating factor (G-CSF) therapy, significantly reduced bacterial loads in the lung and improved disease outcomes. This data reveals that neutrophils play an important ongoing role in confining *S. aureus* to the upper respiratory tract and highlights the use of approaches that improve neutrophil function as effective strategies to treat and reduce the severity of disease in patients at risk of disseminated *S. aureus* infections.

## *RESULTS*

### *Strain dependent variation in the longevity of persistence of nasal S. aureus infection*

To explore immune factors involved in preventing the dissemination of *S. aureus* from the upper to the lower airways we firstly established a mouse model of *S. aureus* nasal carriage. To do this, $10^8$ CFU of a common laboratory strain of *S. aureus* (Newman) was applied to the nares of C57BL/6 mice in a volume of 10 µl, to limit the bacteria to the upper respiratory tract, and at various time points post infection. (p.i.) the bacterial load in the nasal and lung tissue was assessed. *S. aureus* was detectable in the nasal tissue and nasal lavage of the majority (~90%) of mice until day 7 post infection p.i. after which the bacterial loads rapidly declined (Fig 1a-b). Importantly, very low levels of bacteria were sporadically isolated from the lung (Fig 1c), demonstrating that our inoculation strategy largely restricts infection to the upper airways with limited spread of the bacteria to the lower respiratory tract.

This article is protected by copyright. All rights reserved

Author Manuscript

Studies have shown that different strains of *S. aureus* vary in their *in vivo* pathogenicity[17,18]. To improve the longevity of *S. aureus* nasal colonisation we trialled infecting mice with a variety of different strains, a strategy which has previously been adopted by others[19-25,26]. C57BL/6 mice were infected intranasally in the upper respiratory tract with $10^8$ CFU of a panel of *S. aureus* strains and on days 3 and 14 p.i. nasal tissue and lungs were harvested to determine bacterial load. None of the strains tested caused severe disease with only a moderate and transient weight loss being observed across all cohorts of mice (Fig. 1d). While we could recover all strains of *S. aureus* from the nasal tissue of mice at day 3 p.i., only one strain, JKD6159 was still detectable in a sizable proportion of mice at day 14 p.i. (Fig 1e-f). To further validate the extended persistence of JKD6159 in the nasal cavity of mice, we infected a larger cohort of mice with this strain and compared its persistence to a widely used laboratory strain (Newman). At day 14 p.i., ~60% of mice infected with the JKD6159 strain were colonized while only 13% of mice infected with the Newman strain still harboured bacteria in their nasal tissue (Fig 1g-h). By day 21 p.i., we could recover *S. aureus* bacteria from the nasal tissue of 33% of mice infected with the JKD6159 strain while only 6% of mice infected with the Newman strain still harboured bacteria in this site (Fig 1g-h). Therefore, the persistence of *S. aureus* within the murine nasal cavity is partly a function of the bacterial strain used.

***Rapid neutrophil infiltration into the nasal airways following infection with a swiftly eradicated S. aureus strain***

As shown above, 7 out of 8 *S. aureus* strains introduced into the nasal passage of wild type (wt) C57BL/6 mice were rapidly dispelled from this mucosal tissue. To gain insight into the factors driving the clearance of *S. aureus* from the nares we infected mice with the short-term colonising Newman strain, and 1 day later, harvested the nasal tissue and performed immunohistochemistry on nasal tissue sections. The vast majority of bacteria resided within the nasal airways, near the nasal epithelium and interestingly, were already surrounded by nucleated cells (Fig 2a-c). Further analysis of these tissue sections confirmed that the majority of the nucleated cells in the airways surrounding *S. aureus* were $Ly6g^+$ neutrophils (Fig 2d-e). Quantitation of the number of neutrophils in the nose and lung following *S. aureus* nasal infection highlighted a subtle but significant increase in the number of neutrophils within these tissues, which peaked at day 3 p.i. and contracted thereafter (Fig 2f-g). Assessment of the influx of other immune cells into the nasal tissue (ie γδ T cells, monocytes, $CD4^+$ T cells, $CD8^+$ T cells) revealed no change above levels present in naïve mice post *S. aureus* infection (data not shown). These data indicate that intranasal infection with *S. aureus* results in transient neutrophils infiltration into the site of infection.

In order to further study the interaction between *S. aureus* and neutrophils in the nasal cavity, we developed a high throughput assay to track bacteria and host cell interactions *in vivo*. To do this, we infected mice in the upper respiratory tract with carboxyfluorescein succinimidyl ester (CFSE) labelled *S. aureus* (Newman) and at 3, 24 and 48 hrs p.i. harvested the nasal lavage, nasal tissue, lung, cervical and mediastinal lymph nodes, and the presence of CFSE labelled *S. aureus* in various cell types and in each organ was measured

This article is protected by copyright. All rights reserved

Author Manuscript

by flow cytometry. At 3 hours p.i., the vast majority of CFSE$^+$ cells in the nasal tissue were Ly6g$^+$, which is consistent with our immunohistochemistry data showing rapid association of neutrophils with the bacteria in the nasal airways (Supplementary figure 1, Fig 2h). To validate that the CFSE$^+$ cells were harbouring bacteria, we fixed, permeabilized and co-stained these cells with an anti-*S. aureus* antibody. We found that the CFSE$^+$ neutrophils did co-stain with the anti-*S. aureus* antibody (Fig 2h). In the nose, the number of CFSE$^+$ neutrophils peaked at 3 hrs p.i. and declined thereafter, falling below our level of detection beyond 24 hrs p.i. (Fig 2i-j). While CFSE$^+$ neutrophils were present in the nasal wash and nasal tissue, they remained below our limit of detection in the lung and lymph nodes (data not shown) suggesting that the bacteria associated neutrophils were not trafficking *S. aureus* to the draining lymphoid tissue. Repeating the above experiment but replacing viable bacteria with heat killed, CFSE labelled *S. aureus* resulted in similar kinetics of accumulation and clearance of CFSE$^+$ neutrophils in the nasal tissue, suggesting that the loss of CFSE$^+$ bacteria was most likely due to clearance of the bacteria by neutrophils, instead of diminished fluorescence due to bacterial division (Supplementary Fig 2a-b).

While these experiments suggested that *S. aureus* almost exclusively associates with neutrophils following intranasal infection (Supplementary figure 1), it was unclear whether the bacteria were intracellular or whether they were adhering to the surface of these cells. To resolve this, we modified our staining approach and measured the proportion of CFSE$^+$ neutrophils that positively stained with the anti-*S. aureus* antibody, without prior permeabilization. The CFSE$^+$ neutrophils that stained positive with the anti-*S. aureus* antibody without permeabilization would reflect cells that are bound by extracellular bacteria, while the CFSE$^+$ neutrophils in this preparation that do not bind the anti-*S. aureus* antibody would identify cells only harbouring intracellular bacteria. Using this strategy, we determined that ~40% of the *S. aureus* associated neutrophils contained intracellular bacteria (Supplementary figure 2c-e). Therefore, intranasal infection with a transiently persisting *S. aureus* strain results in rapid neutrophils infiltration and bacterial engulfment in the nasal airways.

***Variation in neutrophil recruitment and bacterial association following infection with S. aureus strains that result in short-term (Newman) and long-term (JKD6159) nasal carriage***

The JKD6159 *S. aureus* strain persisted longer and with greater efficiency than any other *S. aureus* strain tested in our study. This strain belongs to the ST93 genotype[18] and has previously been shown to cause severe skin infection[18] and necrotizing pneumonia in humans [27]. To gain insight into why the JKD6159 strain exhibited improved persistence, we examined where the bacteria localized in the nasal airways. To this end, mice were infected in the upper airways with the JKD6159 strain and 1 day later, nasal tissue was recovered, and sections were stained with anti-*S. aureus* and anti-Ly6g to identify bacteria and neutrophils, respectively. At this time point the vast majority of JKD6159 bacteria were residing within the nasal airway, which was similar to our previous observation with the short-term colonising Newman strain (Fig 3a). However, unlike the Newman infection, where the bacteria in the airways were surrounded by Ly6g$^+$

This article is protected by copyright. All rights reserved

Author Manuscript

neutrophils, limited neutrophil association was observed following JKD6159 infection (Fig 3a). To validate this observation, we quantitated the number of neutrophils in the nasal airways and nasal tissue following infection with either Newman or JKD6159 strains. We found that although there were similar numbers of neutrophils in the nasal tissue following infection with either strain, there was a significant reduction in the number of neutrophils egressing into the nasal airways following infection with the JKD6159 strain (Fig 3b-c). Next, we infected mice in the upper respiratory tract with CFSE labelled *S. aureus* JKD6159 or Newman and compared 3 hrs later, the number of bacteria associated neutrophils in the nasal wash and nasal tissue. While we did not observe any difference in the total number of neutrophils in the nasal tissue of JKD6159 or Newman infected mice, which is consistent with our earlier experiments, we did once again, observe significantly fewer neutrophils in the nasal airways of JKD6159 infected mice (Fig 3d-e). Moreover, there were fewer $CFSE^{+}$ neutrophils in both the nasal airways and nasal tissue following infection with the CFSE-JKD6159 strain in comparison to what was observed following infection with the CFSE-Newman strain (Fig 3f-g), suggesting that either neutrophils did not efficiently associate with the JKD6159 strain or potentially, the JKD6159 strain was very effectively lysing the neutrophils following association. A comparison of the level of a panel of inflammatory cytokines/chemokines (interferon gamma (IFNγ), interleukin (IL-) 6, IL-10, IL-12, MCP-1, tumour necrosis factor (TNF) and CXCL1(KC)) in the nasal lavage of mice 3 hrs p.i. with either the JKD6159 or Newman strain revealed significantly reduced inflammatory molecules in the nasal lavage recovered from JKD6159 infected mice (Fig 3h). Of particular relevance, the level of CXCL1, a major neutrophil chemoattractant in mice[28], was significantly reduced in the nasal lavage recovered from JKD6159 infected mice. These data show that infection of mice with the JKD6159 strain provokes less nasal inflammation, evokes less neutrophil egress and association in the nasal airways and this may, in part, be contributing to the enhanced persistence of this strain within the nasal tissue.

***MyD88 signalling mediates neutrophil recruitment into the airways following S. aureus infection***

Previous reports have shown that MyD88 signalling is required for neutrophil recruitment to the skin following a localized *S. aureus* infection[29]. To test whether MyD88 signalling was also involved in neutrophil recruitment into the airways during *S. aureus* nasal infection, MyD88 knockout (KO) mice and wild type (wt) mice were infected in the upper respiratory tract with *S. aureus* (Newman), and from days 1-4 p.i., we quantitated the number of neutrophils infiltrating the airways and respiratory tissue. We observed that at day 1 p.i., in comparison to the wt control cohort, MyD88 KO mice had significantly fewer neutrophils present in the upper (nasal lavage) and the lower (BALf) airways and a reduction in the lung tissue (Fig 4a-d, l). However, by day 2-3 p.i. similar numbers of neutrophils were present in both the airways and respiratory tissue of both cohorts of mice (Fig 4a-d). Next, we measured the level of a panel of cytokines/chemokines in the BALf and found that at 3 hr p.i., MyD88 deficient mice had significantly decreased levels of the neutrophil chemoattractant, CXCL1 (Fig 4e-k). Thus, the lag in neutrophil

This article is protected by copyright. All rights reserved

Author Manuscript

infiltration observed in MyD88 deficient mice may in part, be due to a delay in the production of chemokines involved in neutrophil recruitment. To determine whether the lag in neutrophil recruitment into the airways of MyD88 KO mice following *S. aureus* infection had an impact on bacterial clearance we infected MyD88 KO and wt mice with *S. aureus* (Newman) and monitored disease progression over time. Consistent with our earlier experiments, wt mice developed a very mild disease post *S. aureus* infection, with the bacteria remaining largely confined to the nasal tissue, and ultimately being cleared from all organs by day 7 p.i. (Fig 4m-p). In contrast, MyD88 KO mice developed a severe and disseminated infection, with *S. aureus* being recoverable from both the nasal tissue and lungs (Fig 4m-p). Bacterial loads in the MyD88 KO mice continued to increase in all organs over the course of the experiment. Knockout mice lost weight, approximately 64% of animals developed physical symptoms of an inner ear infection (i.e. head tilt) and by day 11 p.i. 100% of MyD88 KO mice had succumbed to the disease (Fig 4m-p). To confirm the systemic dissemination of *S. aureus* following infection of MyD88 deficient mice, KO and wt mice were infected in the upper airways with a bioluminescent expressing *S. aureus* (JKD6159-LUX) and bacterial dissemination was tracked using an IVIS whole animal imaging system. On day 7 p.i., a strong bioluminescent signal was detected in the inner ear and along the respiratory tract (Fig 4q) as well as in several internal organs (ie. liver, spleen, gut; data not shown) of MyD88 KO mice. In contrast, no luminescent signal was detectable in the wt animals (Fig 4q). These data demonstrate that MyD88 deficient mice have a severe defect in bacterial clearance which is coupled with an early delay in neutrophil influx into the airways.

***Neutrophils block the dissemination of S. aureus from the upper airways into the lung***

Neutrophils respond to *S. aureus* nasal infection by rapidly infiltrating the nasal airways and engulfing the bacteria. We next assessed whether neutrophils play a direct role in preventing the dissemination of *S. aureus* from the nasal tissue. To this end, we depleted neutrophils in C57BL/6 mice via treatment with an anti-Ly6g (1A8) monoclonal antibody on the day prior to inoculation and then every second day over the course of the infection. This regime effectively and systemically depletes neutrophils (Fig 5a-c). At day 3 p.i. similar levels of bacteria were recovered from the nasal tissue of both depleted, and non-depleted control mice, and while depleted animals had significantly higher bacterial load in the nasal tissue at day 7 p.i., by day 14 p.i. the bacterial load returned to a similar level in both groups. Interestingly, bacteria were detectable in the lungs of mice only after neutrophil depletion (Fig 5d-e). Utilizing bioluminescent bacteria and our *in vivo* imaging system we also observed that in addition to allowing bacterial movement into the lung, neutrophil depletion resulted in the transmission of the bacteria into the inner ear in 62% of anti-Ly6g treated animals (Fig 5f). Next, we determined whether neutrophils also played an ongoing role in confining *S. aureus* to the upper airways. Mice were infected in the upper respiratory tract with the JKD6159 strain and following stabilisation of the infection (day 7 p.i.) we began neutrophil depletion by administering the anti-Ly6g monoclonal antibody, which we then readministered every second day to maintain the animals

This article is protected by copyright. All rights reserved

Author Manuscript

in a neutropenic state. On day 7 p.i., prior to the commencement of neutrophil depletion, in a separate cohort of mice, we checked bacterial load and detected CFU counts in the nose but not the lung tissue (Fig 5g-h). We next measured the bacterial burden on day 14 p.i. in the lung and nasal tissue of neutrophil depleted mice and found that these animals displayed a higher bacterial burden in the nose compared to that present in the control non-depleted group (Fig 5g). Moreover, these bacterial loads were also higher than that observed on day 7 p.i. indicating that neutrophil depletion exacerbated infection within the nasal tissue. Interestingly, once again, we could also detect bacteria in the lung in 70% of neutrophil depleted animals (Fig 5h). Collectively, these data show that neutrophils block the dissemination of *S. aureus* from the upper airways into the lung and inner ear and prevent the development of bacterial pneumonia.

***G-CSF treatment boosts neutrophil activity and reduces the severity of influenza induced S. aureus pneumonia***

Neutropoenia and neutrophil disfunction can also occur following infection with various pathogens, after administration of various drugs or after cancer chemotherapy[30,31]. We next examined whether a more physiologically relevant method of neutrophil impairment could also evoke dissemination of nasal *S. aureus* infection. Previous studies have shown that neutrophil dysfunction caused by influenza infection [32] can lead to staphylococcal secondary bacteria pneumonia [33]. Therefore, we investigated whether influenza virus infection can cause *S. aureus* to disseminate from the upper to the lower airways and whether treatments to restore neutrophil function could improve disease outcomes.

Naïve mice, or mice infected intranasally with $10^4$ PFU of influenza A virus (x31, H3N2) 7 days earlier, were infected in the upper respiratory tract with the JKD6159 strain and the bacterial load in the nasal tissue and lung were measured 3 days later (Fig 6a). The nasal tissue from mice concomitantly infected with influenza virus and *S. aureus* harboured a bacterial load 100-fold higher than that observed in mice infected with *S. aureus* alone (Fig 6b). In addition, while no bacteria were present in the lung tissue recovered from mice infected only with *S. aureus*, 77% of the dual infected mice contained bacteria in the lung tissue (Fig 6c). Thus, consistent with prior studies[23,33], we find that preceding influenza virus infection can lead to the development of staphylococcal pneumonia.

We next tested whether boosting neutrophil number/function could limit bacterial dissemination and reduce disease severity in this influenza induced bacteria pneumonia model. We prophylactically treated mice co-infected with influenza virus and *S. aureus* (as described above) with granulocyte colony stimulating factor (G-CSF), a glycoprotein that boosts neutrophil number and function and assessed how this impacted the disease severity and the bacterial load (Fig 6d). We first examined the number and quality of neutrophils in the lung and nasal tissue of G-CSF treated, dual infected mice. While on day 1 post *S. aureus* challenge, we found no significant numerical difference in the number of neutrophils in the nose and lung of dual infected mice with or without G-CSF treatment (Fig 6e-f), we did observe differences in neutrophil

This article is protected by copyright. All rights reserved

Author Manuscript

functionality. Assessment of the expression level of CD69, a marker used to track neutrophil activation revealed that neutrophils recovered from both the nose and lung tissue of G-CSF treated mice had significantly higher expression of this marker compared to untreated controls (Fig 6g-h). We also measured the level of reactive oxygen species (ROS) in these neutrophils by incubating lung cells with $H_2$DCF which, in the presence of $H_2O_2$, oxidises to the green fluorescent product, DCF. Lung neutrophils from G-CSF treated dual infected mice showed a significant increase in the mean fluorescence intensity of intracellular DCF as compared to the levels detected in neutrophils recovered from dual infected mice not subjected to G-CSF therapy (Fig 6i). Finally, we checked whether G-CSF therapy of co-infected mice impacted the bacterial load and the disease outcome. While G-CSF treatment of influenza and *S. aureus* co-infected mice did not impact the levels of bacteria in the nasal tissue (Fig 6j) it did result in a 27-fold reduction in bacteria in the lung (Fig 6k). The depletion of neutrophils (anti-Ly6g) from these G-CSF treated dual infected mice abrogated the reduction of bacteria in the lung, validating that the improvement in disease outcome was neutrophil mediated (Fig 6k). Further monitoring of the G-CSF treated mice showed that they exhibited a more rapid recovery and weight gain compared to dual infected mice that were left untreated (Fig 6l). These data show that approaches to improve neutrophil function may represent alternative strategies to attenuate morbidity associated with *S. aureus* pneumonia.

Author Manuscript

## DISCUSSIONS

*Staphylococcus aureus* is considered to be a human commensal microbe, asymptomatically colonizing the nasal cavity of ~30% of individuals[34]. However, given the opportunity, *S. aureus* can disseminate to cause severe disease, and it is a leading cause of both hospital- and community-acquired infections worldwide. Currently, understanding around the role that the host immune system plays during the transition of *S.*

This article is protected by copyright. All rights reserved

*aureus* from harmless commensal, to disseminated pathogen, is very limited. Here we show that neutrophils play a key role in preserving the balance, and actively confin *S. aureus* to the upper respiratory tract.

Patients with neutrophil deficiencies have a high risk of invasive *S. aureus* infections[15,35]. While prophylactic antibiotic treatment of patients with neutropenia is widely used as a clinical management strategy to prevent staphylococcal infections [36], this approach has many drawbacks, including the capacity to foster the emergence of antibiotic resistance. Data generated in our mouse model would support the use of alternative approaches that enhance neutrophil function in patients at risk of disseminated *S. aureus* infections. Neutrophils can respond to invasive *S. aureus* infection, rapidly being recruited to the site of infection and assisting in bacteria eradication[37,38]. Here we showed that while the nasal airways are largely devoid of neutrophils during the steady state, introduction of *S. aureus* into the upper respiratory tract triggered an extremely rapid influx of these granulocytes into the air space where they co-associated with the bacteria. Depletion of neutrophils alone from mice with *S. aureus* nasal carriage was sufficient to trigger the development of an invasive infection with *S. aureus* spreading from the nasal tissue into the inner ear and lung. This finding was surprising as neutrophils are classically thought of as a rapid and transient first line of defence, while here we show these cells have an ongoing role in preventing the development of an invasive infection. These findings suggest that neutrophils actively preserve respiratory health by keeping nasal commensals confined to the upper airways.

Investigations on neutrophil and *S. aureus* interactions using *in vivo* mouse models have limitations, specifically, many of *S. aureus* immune evasion mechanisms seen in humans fail to operate effectively in the murine host[39-42]. *S. aureus* has evolved an arsenal of factors aimed at evasion of the innate immune system, a significant proportion of which defend against neutrophils[43-48]. The significant redundancy in the numerous mechanisms employed by *S. aureus* to evade neutrophils reflects the importance of these cells in bacterial defence. Of particular relevance*, S. aureus* can cause lysis of human neutrophils following phagocytosis[43,49], however this attack mechanism is ineffective in mouse neutrophils. *S. aureus* is also capable of surviving within human neutrophils, thereby concealing itself and preventing clearance by other phagocytes[50,51] and once again, this immune evasion mechanism is not observed with murine neutrophils. Our murine data highlights the effectiveness of neutrophils at eradicating *S. aureus* in a situation where *S. aureus* is rendered incapable of defending against the antimicrobials produced by these cells. Thus, approaches whereby the killing capacity of human neutrophils are boosted, coupled with therapies that counteract the immune evasion mechanisms of *S. aureus,* may represent an effective treatment for invasive infection.

Utilizing a model of influenza induced staphylococcal pneumonia we showed that prophylactic treatment with G-CSF, a potent enhancer of neutrophil number and function, attenuated the severity of influenza induced *S. aureus* pneumonia. This finding is consistent with previous studies which show that following intrabronchial delivery of *S. aureus,* G-CSF therapy boosts neutrophil numbers, augments bacterial

This article is protected by copyright. All rights reserved

Author Manuscript

clearance, reduces lung injury and improves survival rates[52,53]. The treatment of invasive *S. aureus* infection using G-CSF therapy is only appears to be effective when the host is neutropenic or when the infection is localised to the respiratory tract [54]. The effectiveness of G-CSF as a clinical treatment option for severe bacterial pneumonia has been trialled before. Early clinical trials show that in severe pneumonia, G-CSF (Filgrastim) treatment increases blood neutrophil levels and while it does not impact mortality rates or length of hospitalization, it does significantly reduce the development of serious complications[55]. The beneficial effects of G-CSF in patients with *S. aureus* pneumonia is believed to be, at least in part, due to the increased circulation and enhanced functionality of neutrophils[56]. It is noteworthy that in the abovementioned clinical trial[55], participants were not stratified into groups based on the causative agent of the bacterial pneumonia which may represent a confounding variable as others have previously reported that the type of bacterial infection is a critical factor that determines the effectiveness of prophylactic G-CSF treatment[52]. These data support the further investigation of G-CSF as a prophylactic therapy in neutropenic patients at risk of *S. aureus* pneumonia. While boosting neutrophil influx into the airways could improve the outcomes of severe bacterial pneumonia, it should be noted that tissue destruction can develop from the hyper-activity of these cells[57-59], therefore any therapeutic approaches that boost neutrophil function need to be regulated, allowing for adequate neutrophil-mediated immune responses without excessive tissue damage.

MyD88 is a cytoplasmic adaptor molecule that plays an essential role in IL-1R/TLR family signalling, the activation of which is critical for pathogen recognition. Here we showed that the rapid influx of neutrophils into the nasal airways following *S. aureus* infection was dependent on MyD88 signalling, which is consistent with previous reports that show it is also critical for neutrophil recruitment to a site of a localized *S. aureus* skin infection[29]. While earlier studies showed that intravenous *S. aureus* infection of MyD88 KO mice was 100% lethal [60], others report in the context of a respiratory infection, MyD88 is dispensable for bacterial clearance [61]. In contrast to this published report, we find that similar to other bacterial pneumonia models[62], upper respiratory tract infection of MyD88 KO mice with *S. aureus* is 100% lethal. Many factors may contribute to the observed differences in experimental outcomes, with the dose, the bacterial strain and the mode of delivery (intranasal versus aerosolized) varying between the two studies. Moreover, the original study by Skerret *et al.,* only profiled MyD88 KO mice until day 4 post *S. aureus* infection and, as we show here, MyD88 KO mice only display severe disease at later time points. The high mortality we observed following intranasal *S. aureus* infection of Myd88 KO mice highlights the importance of this signalling molecule in the elimination of invasive *S. aureus* infections.

To develop an effective strategy for the treatment of invasive *S. aureus* infection, it is important to understand both pathogen-related and host-related elements that lead to morbidity and mortality [63]. Here we report that following an upper respiratory tract infection, different strains of *S. aureus* evoke varying

This article is protected by copyright. All rights reserved

Author Manuscript

levels of inflammation. Of the eight *S. aureus* genotypes examined, only the JKD6159 strain was able to persist in the nares of C57BL/6 mice. This isolate evoked less inflammation and did not efficiently associate with neutrophils. The strain JKD6159 is from the dominant CA-MRSA lineage circulating in Australia. Sequence type (ST) 93 likely arose in the 1970s[64,65], with multiple acquisitions of different SCC*mec* cassettes predicted to have occurred in the late 1990s. The JKD6159 strain belongs to the predominant SCC*mec*IVa group (ST93-IV), which is one of the most virulent circulating CA-MRSA clones [18], explained at least in part, by the high level production of alpha toxin and leukocidins[66]. Obtaining a greater understanding of the molecular basis for the colonisation phenotype of ST93-IV isolates (e.g. adhesion, immune evasion and dissemination) will see the development novel *S. aureus* decolonization strategies.

*S. aureus* remains a major cause of human infections, and the rise of highly pathogenic, antibiotic-resistant strains is making treatment increasingly difficult. As the overall burden of disease continues to increase, there is an urgent need for alternative therapeutic approaches against this opportunistic pathogen. Here, we show that neutrophils play an active and essential role in confining *S. aureus* to the nasal tissue and in doing so, they block the development of invasive *S. aureus* infections. Therapies that enhance neutrophil function in patients at risk of disseminated *S. aureus* infections may represent effective strategies to attenuate morbidity associated with staphylococcal pneumonia.

Author Manuscript

## METHODS

Ethics statement

This article is protected by copyright. All rights reserved

All experiments were done in accordance with the Institutional Animal Care and Use Committee guidelines of the University of Melbourne and were approved by the University of Melbourne AEC (APP1714249)

Mice and infections

Female (6-14 week-old) C57BL/6 (CD45.2) and Myd88 KO mice were bred in-house and housed in specific pathogen-free conditions in the Biological Research Facility (BRF) at the Doherty Institute for Infection and Immunity, the University of Melbourne. All mouse strains used were shown not to carry *S. aureus* in the nasal passage. Mice were infected intranasally with $10^4$ PFU of influenza A virus X31 (H3N2) in a volume of 30 µl. Mice were infected intranasally with $10^8$ CFU of *S. aureus* in a volume of 10 µl. Mice were monitored daily for the duration of the experiment starting from day 0 post infection. A mouse losing >15% of body weight, showing signs of respiratory distress, or showing the signs of severe inner ear infection (head tilting and neurological signs) were classified as moribund and were euthanised.

Preparation of *S. aureus* for intranasal inoculation

Streptomycin resistant clones of each *S. aureus* strain used (see Table 1) were isolated in single step selection after overnight growth in Brain Heart infusion (BHI) broth. Each culture was concentrated 10-fold and plated onto BHI agar containing 500 µg/ml of streptomycin. The stability of the resistance was determined after overnight growth of a resistant colony in BHI in the absence of streptomycin and then plating onto BHI agar. A total of 50 colonies from each strain were patched onto BHI agar and BHI agar containing 500 µg/ml of streptomycin. For each strain, all 50 colonies picked were resistant to streptomycin. For Newman we confirmed that the mutation mapped to the *rpsL* gene by whole genome sequencing, yielding a mutation known to confer high level streptomycin resistance in *Bacillus subtilis* (*rpsL*$^{K56N}$) [67]. *S. aureus* were grown at 37°C in a shaking incubator (240 rpm) in BHI supplemented with 100 µg/ml of streptomycin. Mid logarithmic phase bacteria were centrifuged (3500 rpm), resuspended, and washed three times in PBS. The concentration of bacteria was estimated with a spectrophotometer by determining the absorbance at 600 nm ($A_{600}$). Colony-forming units (CFUs) were verified by plating dilutions of the inoculum onto BHI agar containing streptomycin (100 µg/ml) and incubating at 37°C overnight.

Construction of bioluminescent *S. aureus*.

To stably tag *S. aureus* with bacterial luciferase for *in vivo* monitoring, we developed a new suicide vector (pIMC10) which would integrate at a neutral site on the *S. aureus* chromosome (pIMC10a)[68]. The vector pIMC10 was constructed by amplifying the multiple cloning site (flanked by *soxR* and *tonB* transcription terminators) and Phelp-*cat* gene with primers IM1170/IM427 on pIMC6 template [69]. This was joined by SOE-PCR to the minimal pUC18 replicon amplified with IM1169 /IM426. The gel extracted 2.13 kb product was treated with SLiCE for 37°C for 30 min and transformed into IM08B (10 µg/ml

This article is protected by copyright. All rights reserved

Author Manuscript

chloramphenicol selection) [70]. Both pIMC10 and internal portion of the *amy* gene (amplified with IM1131/IM1132 from JKD6159 genomic DNA) were digested with SphI/BglII, gel extracted, ligated and transformed into IM08B, yielding pIMC10a. We chose the immunodominant staphylococcal antigen IsaA to drive luciferase expression due to the strong promoter activity observed with a P*isaA*-YFP fusion [71]. The *isaA* promoter was amplified with primers IM1220/IM654 and the LUX operon with primers IM320/IM1100 on pIMK2lux template [72]. Both amplimers were gel extracted and used as a template for SOE-PCR with IM1220/IM1100, digested with restriction enzymes in the MCS (SalI/NotI) and ligated into complementary digested vector. The new vector pIMC10a(P*isaA*-LUX) was electroporated into JKD6159Δ*hsdR* Δ*hsdR*$^{SCC}$ with selection on BHI agar containing 10 µg/ml chloramphenicol. The integrated plasmid was then transduced into JKD6159$^{STR}$ with phage 11 as described previously [73] to generate strain JKD6159-LUX. Oligonucleotides used in this study are listed in Supplementary table 1.

Flow cytometry

Mice underwent cardiac perfusion before harvest of the lung and nasal tissue. The nasal tissue, including the nasal cavity, nasal turbinates, and NALTs, was obtained by cutting down the vertical plane of the skull and scraping out the tissues and small bones from both sides of the nasal passages. Lung and nasal tissue were enzymatically digested for 1 h at 37 °C in 3 ml of collagenase type 3 (3 mg ml$^{-1}$ in RPMI-1640 supplemented with 2% fetal calf serum). Single cell suspensions were surface stained for 25 min on ice with the appropriate mixture of mAbs. The conjugated mAbs were obtained from BD Pharmingen or BioLegend, or eBioscience (San Diego, CA) include, mouse: anti-Ly6G (1A8) and anti-CD11b (M1/70). Samples were acquired using a Becton Dickinson Fortessa III flow cytometer and data analysed using the FlowJo software package (Tree Star, Inc., Ashland, OR, USA).

Enumeration of *S. aureus* in organs

To evaluate bacterial load, lung and nasal tissue were harvested into 1 ml PBS, homogenized and serial dilutions of organ homogenates were made, plated onto streptomycin containing brain heart infusion (BHI) agar plates, and incubated overnight at 37°C.

Cytokine production in bronchial alveolar lavage (BALf) and nasal lavage fluid

For collection of the nasal lavage the trachea was exposed and cannulated and 300 µl of PBS was flushed through the nasal airways and collected from the nostrils. To collect the BALF, the trachea was exposed and cannulated and the lungs were lavaged three times with 300 µl of PBS. Cytokine/chemokine concentrations in BALf and nasal lavage was measured using LEGENDplex mouse anti-virus response standard panel (Biolegend, San Diego, CA) or a BD Mouse Inflammation cytometric bead array (BD, San Diego, CA) following manufacturer's instructions.

This article is protected by copyright. All rights reserved

Author Manuscript

*In vivo* Ly6G depletion and G-CSF treatment

To deplete neutrophils mice were administered via intraperitoneal injection, 500 µg of anti-Ly6G (1A8, Bio X Cell, West Lebanon, NH) or a control anti-rat IgG, the day before infection and then every second day thereafter for the duration of the experiment.

G-CSF treatment: Mice were given via intraperitoneal injection 200 ng of recombinant murine GCSF (Miltenyi Biotec, Bergisch Gladbach, Germany) daily for the duration of the experiment.

*Measurement of intracellular ROS*

Lung cells were assessed for intracellular hydrogen peroxide ($H_2O_2$) using an DCFDA/H2DCFDA cellular ROS assay kit following manufacturer's instructions (Abcam, Cambridge, MA, USA). Briefly, lung cells were cultured with Fluorescent 6-carboxy-2'7'-dichlorofluorescien diacetate, di(acetoxymethlyl ester) which is taken up by cells and in the presence of $H_2O_2$ is oxidized to the green florescent product 2'7'-dichlorofluorescein (DCF). DCF is then trapped within the cells and is detectable by flow cytometry. $H_2$DCF (20 µM) was added to cells and incubated for 30 minutes at either 4°C (background levels of fluorescence) or 37°C and DCF levels in neutrophils were determined by flow cytometry.

*S. aureus* labelling with carboxyfluorescein diacetate succinimidyl ester (CFSE)

*S. aureus*, grown in 10 ml BHI broth with 100 µg/ml streptomycin (Sigma, Santa Clara, CA, USA) to an $OD_{600}$ of 1.0 was pelleted at 3500 rpm for 10 mins, and resuspended in 10 ml of 10 µM CFSE in PBS. Bacteria was incubated at 37 °C in dark for 1 hour, while shaking to ensure bacteria were evenly stained. After staining, bacteria were washed in 10 ml PBS three times. Mice were infected intranasally with $10^8$ CFUs of CFSE labelled *S. aureus*. Nasal wash and nasal tissue were harvested at different timepoints post-infection and the proportion of bacteria that were intracellularly or extracellularly associated with different immune cells was measured by flow cytometry. To identify cells harbouring intracellular bacteria, single cell suspensions of nasal tissue and nasal wash samples were surface stained with immune cell markers (CD11b, Ly6G) and anti-*S. aureus* polyclonal antibody (ThermoFisher, Waltham, MA, USA, Cat#PA1-7246) – in this case only the extracellular bacteria would be labelled with anti-*S. aureus* antibody, and thus any $CFSE^+$ cells which stain negative for anti-*S. aureus* would represent cells that contain intracellular *S. aureus*. Alternatively, the single cell suspensions were stained with CD11b and Ly6G first, then fixed and permeabilised, and stained for both intracellular and extracellular *S. aureus* using the anti-*S. aureus* antibody.

Quantification of *in vivo S. aureus*: *in vivo* bioluminescence

*In vivo* imaging of live animals was performed using the IVIS 200 imaging system (Caliper Life Sciences). Imaging was performed for 5 min, during which time isoflurane was pumped into the imaging chamber at

This article is protected by copyright. All rights reserved

Author Manuscript

a rate of 0.5 L/min. Images were analyzed using the Living Image 3.0 software package (Caliper Life Sciences). Data are presented on colour scale overlaid on a grey-scale photograph of mice.

Immunohistochemistry

Euthanized mice were decapitated, their heads were skinned, and the lower jaws, including tongue, were removed. Tissue was fixed in 4% paraformaldehyde for 4 hours on ice, washed twice with PBS, and incubated with agitation for 72 hours at room temperature in 20% EDTA (pH = 7.5). Tissue was embedded in optimum cutting temperature, and frozen sections (14 μm) were cut using a cryostat. Tissue sections were fixed with acetone and blocked in serum-free protein block (DAKO, Santa Clara, CA ). Sections were stained with a polyclonal rabbit anti-*S. aureus* antibody (ThermoFisher, Waltham, MA, USA, Cat#PA1-7246), anti-mouse Ly6G(1A8)-Alexa647 and DAPI. The coverslips were mounted in Prolong Gold Antifade medium. Slides were imaged using a Zeiss LSM700 microscope and images were analysed using ImageJ (version 2).

Statistical analysis

Data were analysed using GraphPad Prism and the indicated statistical tests as stated in the figure legend. * $P < 0.05$, ** $P < 0.01$, *** $P < 0.001$, ****$P < 0.0001$.

**FUNDING**: This work was supported by National Health and Medical Research Council of Australia (LMW) and CG was supported by the China Scholarship Council (CG). **AUTHOR CONTRIBUTION**: LMW and IM designed the project with input from TS. Experiments and data analysis were performed by LMW, IM, CG, SM and JB. **COMPETING INTEREST**: The authors declare that they have no competing interests

Author Manuscript

This article is protected by copyright. All rights reserved

## REFERENCES


1. Sakr A, Bregeon F, Mege JL, Rolain JM, Blin O. *Staphylococcus aureus* Nasal Colonization: An Update on Mechanisms, Epidemiology, Risk Factors, and Subsequent Infections. *Front Microbiol* 2018; **9**: 2419.
2. Breuer K, S HA, Kapp A, Werfel T. *Staphylococcus aureus*: colonizing features and influence of an antibacterial treatment in adults with atopic dermatitis. *Br J Dermatol* 2002; **147**: 55-61.
3. Kluytmans J, van Belkum A, Verbrugh H. Nasal carriage of *Staphylococcus aureus*: epidemiology, underlying mechanisms, and associated risks. *Clin Microbiol Rev* 1997; **10**: 505-520.
4. Boucher HW, Corey GR. Epidemiology of methicillin-resistant *Staphylococcus aureus*. *Clin Infect Dis* 2008; **46 Suppl 5**: S344-349.
5. System N. National Nosocomial Infections Surveillance (NNIS) System Report, Data Summary from January 1990-May 1999, issued June 1999. A report from the NNIS System. *Am J Infect Control* 1999; **27**: 520-532.
6. Wertheim HF, Vos MC, Ott A*, et al.* Risk and outcome of nosocomial *Staphylococcus aureus* bacteraemia in nasal carriers versus non-carriers. *Lancet* 2004; **364**: 703-705.
7. Klevens RM, Morrison MA, Nadle J*, et al.* Invasive methicillin-resistant *Staphylococcus aureus* infections in the United States. *JAMA* 2007; **298**: 1763-1771.
8. von Eiff C, Becker K, Machka K, Stammer H, Peters G. Nasal carriage as a source of *Staphylococcus aureu*s bacteremia. Study Group. *N Engl J Med* 2001; **344**: 11-16.
9. Rubinstein E, Kollef MH, Nathwani D. Pneumonia caused by methicillin-resistant *Staphylococcus aureus*. *Clin Infect Dis* 2008; **46 Suppl 5**: S378-385.
10. Jacobs DM, Shaver A. Prevalence of and outcomes from *Staphylococcus aureus* pneumonia among hospitalized patients in the United States, 2009-2012. *Am J Infect Control* 2017; **45**: 404-409.
11. Vardakas KZ, Matthaiou DK, Falagas ME. Incidence, characteristics and outcomes of patients with severe community acquired-MRSA pneumonia. *Eur Respir J* 2009; **34**: 1148-1158.
12. Vardakas KZ, Matthaiou DK, Falagas ME. Comparison of community-acquired pneumonia due to methicillin-resistant and methicillin-susceptible *Staphylococcus aureus* producing the Panton-Valentine leukocidin. *Int J Tuberc Lung Dis* 2009; **13**: 1476-1485.
13. Williams DJ, Hall M, Brogan TV*, et al.* Influenza coinfection and outcomes in children with complicated pneumonia. *Arch Pediatr Adolesc Med* 2011; **165**: 506-512.
14. Craig A, Mai J, Cai S, Jeyaseelan S. Neutrophil recruitment to the lungs during bacterial pneumonia. *Infection and immunity* 2009; **77**: 568-575.


This article is protected by copyright. All rights reserved

Author Manuscript

15. Rigby KM, DeLeo FR. Neutrophils in innate host defense against *Staphylococcus aureus* infections. *Semin Immunopathol* 2012; **34**: 237-259.
16. Robertson CM, Perrone EE, McConnell KW*, et al.* Neutrophil depletion causes a fatal defect in murine pulmonary *Staphylococcus aureus* clearance. *J Surg Res* 2008; **150**: 278-285.
17. van Belkum A, Melles DC. Not all Staphylococcus aureus strains are equally pathogenic. *Discov Med* 2005; **5**: 148-152.
18. Chua KY, Seemann T, Harrison PF*, et al.* The dominant Australian community-acquired methicillin-resistant *Staphylococcus aureus* clone ST93-IV [2B] is highly virulent and genetically distinct. *PloS one* 2011; **6**: e25887.
19. Gonzalez-Zorn B, Senna JP, Fiette L*, et al.* Bacterial and host factors implicated in nasal carriage of methicillin-resistant *Staphylococcus aureus* in mice. *Infection and immunity* 2005; **73**: 1847-1851.
20. Cowan ST, Shaw C, Williams RE. Type strain for *Staphylococcus aureus* Rosenbach. *J Gen Microbiol* 1954; **10**: 174-176.
21. Sahibzada S, Abraham S, Coombs GW*, et al.* Transmission of highly virulent community-associated MRSA ST93 and livestock-associated MRSA ST398 between humans and pigs in Australia. *Sci Rep* 2017; **7**: 5273.
22. Kuroda M, Ohta T, Uchiyama I*, et al.* Whole genome sequencing of meticillin-resistant *Staphylococcus aureus*. *Lancet* 2001; **357**: 1225-1240.
23. Planet PJ, Parker D, Cohen TS*, et al.* Lambda Interferon Restructures the Nasal Microbiome and Increases Susceptibility to *Staphylococcus aureus* Superinfection. *MBio* 2016; **7**: e01939-01915.
24. Desbois AP, Sattar A, Graham S, Warn PA, Coote PJ. MRSA decolonization of cotton rat nares by a combination treatment comprising lysostaphin and the antimicrobial peptide ranalexin. *J Antimicrob Chemother* 2013; **68**: 2569-2575.
25. Mulcahy ME, Geoghegan JA, Monk IR*, et al.* Nasal colonisation by *Staphylococcus aureus* depends upon clumping factor B binding to the squamous epithelial cell envelope protein loricrin. *PLoS Pathog* 2012; **8**: e1003092.
26. Kiser KB, Cantey-Kiser JM, Lee JC. Development and characterization of a *Staphylococcus aureus* nasal colonization model in mice. *Infection and immunity* 1999; **67**: 5001-5006.
27. Chua K, Seemann T, Harrison PF*, et al.* Complete genome sequence of *Staphylococcus aureus* strain JKD6159, a unique Australian clone of ST93-IV community methicillin-resistant *Staphylococcus aureus*. *J Bacteriol* 2010; **192**: 5556-5557.
28. Balamayooran G, Batra S, Fessler MB, Happel KI, Jeyaseelan S. Mechanisms of neutrophil accumulation in the lungs against bacteria. *Am J Respir Cell Mol Biol* 2010; **43**: 5-16.

This article is protected by copyright. All rights reserved

Author Manuscript

29. Miller LS, O'Connell RM, Gutierrez MA*, et al.* MyD88 mediates neutrophil recruitment initiated by IL-1R but not TLR2 activation in immunity against *Staphylococcus aureus. Immunity* 2006; **24**: 79-91.
30. Moore DC. Drug-Induced Neutropenia: A Focus on Rituximab-Induced Late-Onset Neutropenia. *P T* 2016; **41**: 765-768.
31. Freifeld AG, Bow EJ, Sepkowitz KA*, et al.* Clinical practice guideline for the use of antimicrobial agents in neutropenic patients with cancer: 2010 Update by the Infectious Diseases Society of America. *Clin Infect Dis* 2011; **52**: 427-431.
32. McNamee LA, Harmsen AG. Both influenza-induced neutrophil dysfunction and neutrophil-independent mechanisms contribute to increased susceptibility to a secondary *Streptococcus pneumoniae* infection. *Infection and immunity* 2006; **74**: 6707-6721.
33. Reddinger RM, Luke-Marshall NR, Hakansson AP, Campagnari AA. Host Physiologic Changes Induced by Influenza A Virus Lead to *Staphylococcus aureus* Biofilm Dispersion and Transition from Asymptomatic Colonization to Invasive Disease. *MBio* 2016; **7**.
34. Gorwitz RJ, Kruszon-Moran D, McAllister SK*, et al.* Changes in the prevalence of nasal colonization with *Staphylococcus aureus* in the United States, 2001-2004. *J Infect Dis* 2008; **197**: 1226-1234.
35. Lekstrom-Himes JA, Gallin JI. Immunodeficiency diseases caused by defects in phagocytes. *N Engl J Med* 2000; **343**: 1703-1714.
36. Leibovici L, Paul M, Cullen M*, et al.* Antibiotic prophylaxis in neutropenic patients: new evidence, practical decisions. *Cancer* 2006; **107**: 1743-1751.
37. Archer NK, Harro JM, Shirtliff ME. Clearance of *Staphylococcus aureus* nasal carriage is T cell dependent and mediated through interleukin-17A expression and neutrophil influx. *Infection and immunity* 2013; **81**: 2070-2075.
38. Schulz A, Jiang L, de Vor L*, et al.* Neutrophil Recruitment to Noninvasive MRSA at the Stratum Corneum of Human Skin Mediates Transient Colonization. *Cell Rep* 2019; **29**: 1074-1081 e1075.
39. Tseng CW, Biancotti JC, Berg BL*, et al.* Increased Susceptibility of Humanized NSG Mice to Panton-Valentine Leukocidin and *Staphylococcus aureus* Skin Infection. *PLoS Pathog* 2015; **11**: e1005292.
40. Reizner W, Hunter JG, O'Malley NT, Southgate RD, Schwarz EM, Kates SL. A systematic review of animal models for *Staphylococcus aureus* osteomyelitis. *Eur Cell Mater* 2014; **27**: 196-212.
41. Kim HK, Missiakas D, Schneewind O. Mouse models for infectious diseases caused by *Staphylococcus aureus*. *J Immunol Methods* 2014; **410**: 88-99.
42. Buer J, Balling R. Mice, microbes and models of infection. *Nat Rev Genet* 2003; **4**: 195-205.
43. Loffler B, Hussain M, Grundmeier M*, et al. Staphylococcus aureus* panton-valentine leukocidin is a very potent cytotoxic factor for human neutrophils. *PLoS Pathog* 2010; **6**: e1000715.
This article is protected by copyright. All rights reserved
Author Manuscript

44. de Haas CJ, Veldkamp KE, Peschel A*, et al.* Chemotaxis inhibitory protein of *Staphylococcus aureus*, a bacterial antiinflammatory agent. *J Exp Med* 2004; **199**: 687-695.
45. Otto M. Basis of virulence in community-associated methicillin-resistant *Staphylococcus aureus*. *Annu Rev Microbiol* 2010; **64**: 143-162.
46. Foster TJ. Immune evasion by staphylococci. *Nat Rev Microbiol* 2005; **3**: 948-958.
47. Postma B, Poppelier MJ, van Galen JC*, et al.* Chemotaxis inhibitory protein of *Staphylococcus aureus* binds specifically to the C5a and formylated peptide receptor. *J Immunol* 2004; **172**: 6994-7001.
48. Goldmann O, Medina E. *Staphylococcus aureus* strategies to evade the host acquired immune response. *Int J Med Microbiol* 2018; **308**: 625-630.
49. Yang D, Ho YX, Cowell LM, Jilani I, Foster SJ, Prince LR. A Genome-Wide Screen Identifies Factors Involved in *S. aureus*-Induced Human Neutrophil Cell Death and Pathogenesis. *Front Immunol* 2019; **10**: 45.
50. Gresham HD, Lowrance JH, Caver TE, Wilson BS, Cheung AL, Lindberg FP. Survival of *Staphylococcus aureus* inside neutrophils contributes to infection. *J Immunol* 2000; **164**: 3713-3722.
51. Thwaites GE, Gant V. Are bloodstream leukocytes Trojan Horses for the metastasis of *Staphylococcus aureus*? *Nat Rev Microbiol* 2011; **9**: 215-222.
52. Karzai W, von Specht BU, Parent C*, et al.* G-CSF during Escherichia coli versus *Staphylococcus aureus* pneumonia in rats has fundamentally different and opposite effects. *Am J Respir Crit Care Med* 1999; **159**: 1377-1382.
53. Sevransky JE, Parent C, Cui X*, et al.* Granulocyte colony-stimulating factor has differing effects comparing intravascular versus extravascular models of sepsis. *J Trauma* 2004; **57**: 618-625.
54. Alp E, Gozukucuk S, Canoz O, Kirmaci B, Doganay M. Effect of granulocyte colony-stimulating factor in experimental methicillin resistant *Staphylococcus aureus* sepsis. *BMC Infect Dis* 2004; **4**: 43.
55. Nelson S, Belknap SM, Carlson RW*, et al.* A randomized controlled trial of filgrastim as an adjunct to antibiotics for treatment of hospitalized patients with community-acquired pneumonia. CAP Study Group. *J Infect Dis* 1998; **178**: 1075-1080.
56. Dale DC, Liles WC, Summer WR, Nelson S. Review: granulocyte colony-stimulating factor--role and relationships in infectious diseases. *J Infect Dis* 1995; **172**: 1061-1075.
57. Bosmann M, Grailer JJ, Ruemmler R*, et al.* Extracellular histones are essential effectors of C5aR- and C5L2-mediated tissue damage and inflammation in acute lung injury. *FASEB J* 2013; **27**: 5010-5021.
58. Xu J, Zhang X, Pelayo R*, et al.* Extracellular histones are major mediators of death in sepsis. *Nature medicine* 2009; **15**: 1318-1321.

This article is protected by copyright. All rights reserved

Author Manuscript

59. Saffarzadeh M, Juenemann C, Queisser MA*, et al.* Neutrophil extracellular traps directly induce epithelial and endothelial cell death: a predominant role of histones. *PloS one* 2012; **7**: e32366.
60. Takeuchi O, Hoshino K, Akira S. Cutting edge: TLR2-deficient and MyD88-deficient mice are highly susceptible to *Staphylococcus aureus* infection. *J Immunol* 2000; **165**: 5392-5396.
61. Skerrett SJ, Liggitt HD, Hajjar AM, Wilson CB. Cutting edge: myeloid differentiation factor 88 is essential for pulmonary host defense against Pseudomonas aeruginosa but not *Staphylococcus aureus*. *J Immunol* 2004; **172**: 3377-3381.
62. Naiki Y, Michelsen KS, Schroder NW*, et al.* MyD88 is pivotal for the early inflammatory response and subsequent bacterial clearance and survival in a mouse model of Chlamydia pneumoniae pneumonia. *J Biol Chem* 2005; **280**: 29242-29249.
63. Mulcahy ME, McLoughlin RM. Host-Bacterial Crosstalk Determines *Staphylococcus aureus* Nasal Colonization. *Trends Microbiol* 2016; **24**: 872-886.
64. Stinear TP, Holt KE, Chua K*, et al.* Adaptive change inferred from genomic population analysis of the ST93 epidemic clone of community-associated methicillin-resistant *Staphylococcus aureus*. *Genome Biol Evol* 2014; **6**: 366-378.
65. van Hal SJ, Steinig EJ, Andersson P*, et al.* Global Scale Dissemination of ST93: A Divergent Staphylococcus aureus Epidemic Lineage That Has Recently Emerged From Remote Northern Australia. *Front Microbiol* 2018; **9**: 1453.
66. Chua KY, Monk IR, Lin YH*, et al.* Hyperexpression of alpha-hemolysin explains enhanced virulence of sequence type 93 community-associated methicillin-resistant *Staphylococcus aureus*. *BMC Microbiol* 2014; **14**: 31.
67. Tojo S, Tanaka Y, Ochi K. Activation of Antibiotic Production in Bacillus spp. by Cumulative Drug Resistance Mutations. *Antimicrob Agents Chemother* 2015; **59**: 7799-7804.
68. Yepes A, Koch G, Waldvogel A, Garcia-Betancur JC, Lopez D. Reconstruction of mreB expression in *Staphylococcus aureus* via a collection of new integrative plasmids. *Appl Environ Microbiol* 2014; **80**: 3868-3878.
69. Kofoed EM, Yan D, Katakam AK*, et al.* De Novo Guanine Biosynthesis but Not the Riboswitch-Regulated Purine Salvage Pathway Is Required for *Staphylococcus aureus* Infection In Vivo. *J Bacteriol* 2016; **198**: 2001-2015.
70. Monk IR, Tree JJ, Howden BP, Stinear TP, Foster TJ. Complete Bypass of Restriction Systems for Major *Staphylococcus aureus* Lineages. *MBio* 2015; **6**: e00308-00315.
71. Monk IR, Shaikh N, Begg SL*, et al.* Zinc-binding to the cytoplasmic PAS domain regulates the essential WalK histidine kinase of Staphylococcus aureus. *Nat Commun* 2019; **10**: 3067.
72. Monk IR, Gahan CG, Hill C. Tools for functional postgenomic analysis of listeria monocytogenes. *Appl Environ Microbiol* 2008; **74**: 3921-3934.

This article is protected by copyright. All rights reserved

Author Manuscript

73. Foster TJ. 7.9 Molecular genetic analysis of staphylococcal virulence. *Method Microbiol* 1998; **27**: 433.

Author Manuscript

Table 1. *S. aureus* strains used in this study

| Bacterial strains | Description | Reference |
|---|---|---|
| Newman | MSSA (CC8) | [25] [26] |
| JKD6159 | CA-MRSA (ST93) | [21] |
| Cowan | MSSA (CC30) | [20] |

This article is protected by copyright. All rights reserved

| | | |
|---|---|---|
| N315 | MRSA (CC5) | Isolated from the pharynx [22] |
| TPS3298 | Isolated from a Rhinosinuitis patient. (CC1) | Laboratory collection |
| COL | HA-MRSA (CC8) | [19] |
| LAC | CA-MRSA CC8 | [23] |
| NRS384 | CA-MRSA CC8 | [24] |

Author Manuscript

**Figure 1: Strain dependent variation in the longevity of persistence of nasal *S. aureus* infection**

(a-c) C57BL/6 mice were infected intranasally in the upper respiratory tract (URT) with $10^8$ CFU of *S. aureus* (Newman) and at the indicated days post infection the bacterial load in the (a) nose, (b) nasal lavage and (c) lung was measured. Dots represent individual mice (n=6-21 mice per timepoint) and the bars

This article is protected by copyright. All rights reserved

represent the mean ± SEM. Data are pooled from 4 independent experiments (d-f) C57BL/6 mice were infected intranasally in the URT with $10^8$ CFU of a panel of *S. aureus* strains (d) average weight loss over the course of the infection and (e) the bacterial load and (f) percentage colonisation in the nasal tissue at day 3 and 14 post infection was measured. Dots represent individual mice (n=3-14 mice per group) and the bar represent the mean. Data are pooled from 2 independent experiments (g-h) C57BL/6 mice were infected intranasally in the URT with $10^8$ CFU of either *S. aureus* Newman or *S. aureus* JKD6159. The bacterial load in the (g) nose and (h) lung at day 3, 14 and 21 post infection were measured. Dots represent individual mice (n=6-21 mice per group) and the bar represent the mean ± SEM. Data are pooled from 3 independent experiments.

**Figure 2: Rapid neutrophil infiltration into the nasal airways following infection with a transiently persisting (Newman) *S. aureus* strain.**

(a-c) Immunofluorescence staining on nasal tissue sections of mice on day 1 post URT infection with *S. aureus* (Newman) stained with anti-*S. aureus* (green) and DAPI (grey) (d-e) Immunofluorescence staining on nasal tissue section of mice on day 1 post URT infection with *S. aureus* (Newman) stained with anti-*S. aureus* (green), anti-Ly6g (pink) and DAPI (grey). Data is representative of 2 independent experiments. (f-g) Mice were infected intranasally in the URT with $10^8$ CFU of *S. aureus* (Newman) and at the indicated days post infection the absolute number of neutrophils ($Ly6g^+CD11b^+$) in the (f) lung and (g) nose was measured. Symbols represent individual mice (n=4-17 mice per time point) and the lines represent the mean ± SEM (one way ANONVA, Sidak's multiple comparison). Data are pooled from 3 independent experiments (h-j) Mice infected intranasally in the URT with $10^8$ CFUs of CFSE labelled *S. aureus* (Newman) were sacrificed at indicated timepoints $CFSE^+$ cells in the nose and nasal lavage was measured by flow cytometry (h) Representative flow cytometry profiles gated on $CFSE^+$ cells in the nasal tissue harvested at 3 hours p.i., staining for Ly6g and anti-*S.aureus*. (i-j) The absolute number of $CFSE^+$ neutrophils in the (i) nasal lavage and (j) nose. Dots represent individual mice (n=4-12 mice per time point). Results are expressed as mean ± SEM. The result is a combination of 3 independent experiments (one way ANONVA, Sidak's multiple comparison).

**Figure 3: Difference in neutrophil recruitment and bacterial association following infection with *S. aureus* strains that results in either short- (Newman) or long- (JKD6159) term nasal carriage**

(a) Immunofluorescence staining on nasal tissue section of mice on day 1 post URT infection with *S. aureus* (JKD6159) staining with a polyclonal anti-*S. aureus* antibody (green) and anti-Ly6g (pink). Data are pooled from 2 independent experiments (b-c) Mice were infected intranasally in the URT with $10^8$ CFU of *S. aureus* Newman or JKD6159 and at the indicated days post infection the absolute number of neutrophils ($Ly6g^+CD11b^+$) in the (b) nose and (c) nasal lavage was measured. Bars represent the mean ± SEM. Data are pooled from 3 independent experiments (n= 5 or 6 per group, two way ANOVA Sidak's multiple

This article is protected by copyright. All rights reserved

Author Manuscript

comparison) (d-g) Mice infected intranasally in the URT with $10^8$ CFUs of CFSE labelled *S. aureus* Newman or JKD6159 were sacrificed at 3 h post infection and flow cytometry was performed to quantitate the total number and the number of $CFSE^+$ neutrophils in the (d,g) nasal tissue and (e-f) nasal lavage. Bars represent the mean ± SEM (n=7-16 mice per group, Mann-Whitney test). Data are pooled from of 3 independent experiments. (h) Cytokine profile of the nasal lavage of either naïve mice or mice 3 h following JKD6159 or Newman infection. Dots represent individual mice with the bars representing the mean ± SEM. Data are pooled from 4 independent experiments (n=5-14, two way ANOVA Tukey's multiple comparison.

**Figure 4: Myd88 signalling facilitates neutrophil recruitment into the airways following *S. aureus* infection.**

(a-d) Myd88 KO and C57BL/6 mice were intranasally infected in the URT with $10^8$ CFUs of *S. aureus* (Newman) and at days 1-4 post infection the number of neutrophils in the (a) nasal lavage (b) nasal tissue (c) lung and (d) bronchial alveolar lavage (BALf) was measured. Data pooled from 5 independent experiments. Symbols represent the mean ± SEM. Data are pooled from 3 independent experiments (n= 4-20 per group, two-way ANOVA Sidak's multiple comparison) (e-k) Myd88 KO and C57BL/6 mice were intranasally infected in the URT with $10^8$ CFUs of *S. aureus* (Newman) and the level of a panel of cytokines/chemokines in the nasal lavage at the indicated times was measured by cytometric bead array. Symbols represent the mean + SEM (n=4-9 mice per time point). Data are pooled from 4 independent experiments. (l) Immunofluorescence staining on nasal tissue section of Myd88 KO mice on day 1 post URT infection with *S. aureus*. (Newman) staining with a polyclonal anti-*S.aureus* antibody (green) and anti-Ly6g (pink). Data is representative of 2 independent experiments (m-p) Myd88 KO and C57BL/6 mice were intranasally infected in the URT with $10^8$ CFUs of *S. aureus* Newman. Mice were sacrificed at indicated timepoints and the bacterial load in the (m) nasal tissue, (n) lung, (o) nasal lavage and (p) BALf were measured. Dots represent individual mice data are pooled from 3 experiments (n=10 mice per group). The dotted line represents the limitation of detection. (q) Myd88 KO and C57BL/6 mice were intranasally in the URT with $10^8$ CFUs of *S. aureus* JKD6159-LUX and were imagined on day 7 p.i. Images are representative of 2 independent experiments. A luminescent signal indicates the presence of live, actively replicating *S. aureus* at the site.

**Figure 5: Neutrophils block the dissemination of *S. aureus* from the upper airways into the lung**

(a-e) Mice were treated with anti-Ly6g antibody one day prior to *S. aureus* URT infection with $10^8$ CFU (Newman) and were treated every second day thereafter for the duration of the experiment. Control mice were treated with an equal volume of PBS. On day 7 post treatment the number of neutrophils in (a) nasal lavage (b) spleen and (c) blood was measured by flow cytometry. Bacterial loads in (d) nasal tissues and (e) lungs were measured on days 3, 5 and 7 post treatment. Results are expressed as mean ± SEM, dots

This article is protected by copyright. All rights reserved

Author Manuscript

represent individual mice (n=7 or 8 mice per group) and results are pooled from 4 independent experiments (two way ANOVA Sidak's multiple comparison) (f) Mice intranasally infected in the URT tract with $10^8$ CFUs of *S. aureus* JKD6159-LUX were treated with anti-Ly6g as described above. Control mice were treated with an equal volume of PBS. Mice were imaged on day 7 p.i. Representative images of 2 independent experiments are shown. A luminescent signal indicates the presence of live, actively replicating *S. aureus* at the site. (g) Mice were treated with anti-Ly6g or PBS at days 7, 9, 11, and 13 post *S. aureus* JKD6159 URT infection with $10^8$ CFU. Bacterial loads in the (g) nasal tissues and (h) lungs of different groups were determined on day 7 (before Ly6g depletion) and 14 p.i. Dots represent individual mice (n=5-10 mice per group) and the lines show the mean ± SEM. The dotted line represents the limitation of detection (one-way ANOVA Sidak's multiple comparison). Data are pooled from 3 independent experiments.

**Figure 6: G-CSF treatment boosts neutrophil function and reduces the severity of influenza induced *S. aureus* pneumonia**

(a-c) C57BL/6 mice were given intranasally either $10^4$ PFU of influenza virus (x31, H3N2) or as a control saline, and 7 days later were infected in the URT with $10^8$ CFUs of *S. aureus* (JKD6159). On day 3 post *S. aureus* infection the bacterial load in the (b) nasal tissue and (c) lung was measured. Dots represent individual mice (n=8-13 mice per group) data are pooled from 3 independent experiments. The dotted line represents the limitation of detection (Mann-Whitney test) (d-l) C57BL/6 mice were given intranasally either $10^4$ PFU of influenza virus (x31, H3N2) or saline as a control, and 7 days later were infected in the URT with $10^8$ CFUs of *S. aureus* (JKD6159). A proportion of the dual infected cohort received G-CSF daily for the duration of the experiment commencing from day 5 post influenza infection. In addition, a proportion of the GCSF treated mice received anti-Ly6g (1A8). (e-f) The absolute number of neutrophils in the (e) lung and (f) nasal tissue of mice on day 1 post *S. aureus* infection. Symbols represent individual mice with the bar representing the mean + SEM. Data are pooled from 4 independent experiments (n=4-12 mice per group). (g-h) The mean fluorescence intensity (MFI) of CD69 on neutrophils recovered from the (g) lung and (h) nose of mice on day 1 post *S. aureus* challenge. Symbols represent individual mice with the bar representing the mean + SEM. Data are pooled from 2 independent experiments (n=6 mice per group, one-way ANOVA Dunnett's multiple comparison). (i) The amount of ROS as measured by MFI of $H_2$DFCDA in neutrophils recovered from the lung of mice on day 1 post *S. aureus* challenge following incubation with 20 μM of $H_2$DFCDA at either 4°C (background) or 37°C for 30 mins. Bars represent the mean + SEM (n=4 mice per group, two-way ANOVA Tukey's multiple comparison). Data are pooled from 2 independent experiments. (j-k) The bacterial load in the (j) nasal tissue and (k) lung was measured on day 3 post *S. aureus* infection. Violin plots show all points which represent individual mice. Data are pooled from 5 independent experiments (n=9-35 mice per group, one-way ANOVA Tukey's multiple comparison) (l) Weight loss measured over the course of the experiment. Symbols represent the mean + sem. Data are

This article is protected by copyright. All rights reserved

Author Manuscript

pooled from 2 independent experiments (n=4 per group, two-way ANOVA Sidak's multiple comparison). The red band indicates the day on which *S. aureus* was administered.

Author Manuscript

This article is protected by copyright. All rights reserved

Figure 1

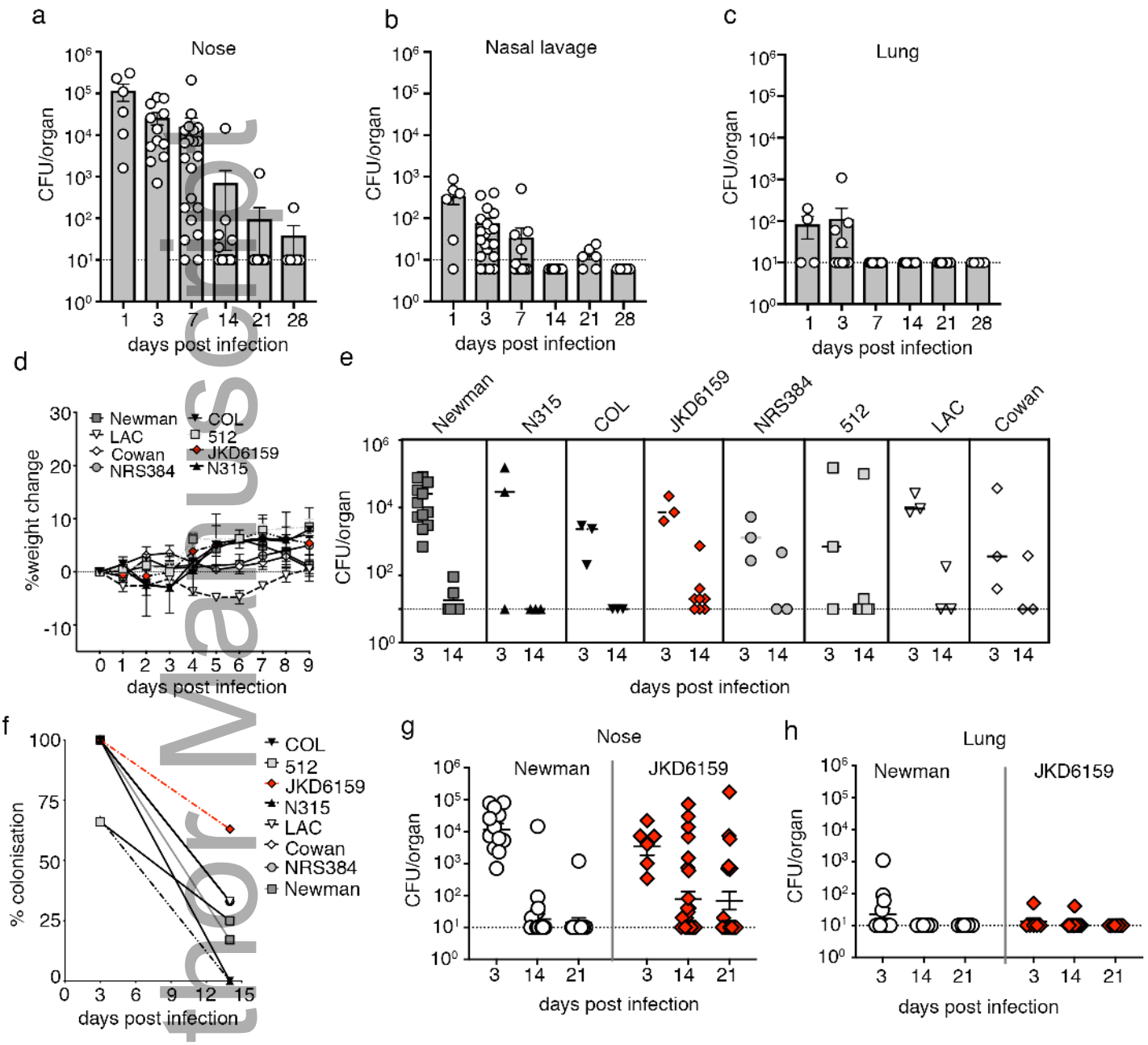


imcb_12343_f1.tif

Author Manuscript

This article is protected by copyright. All rights reserved

Author Manuscript

Figure 2

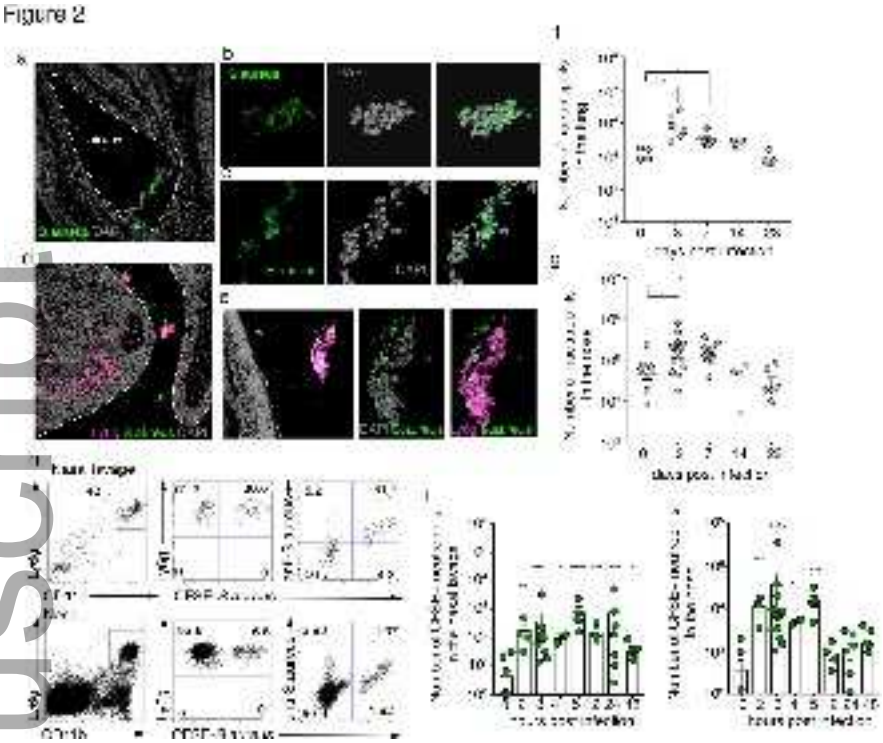

imcb_12343_f2.tif

This article is protected by copyright. All rights reserved

Author Manuscript

Figure 3

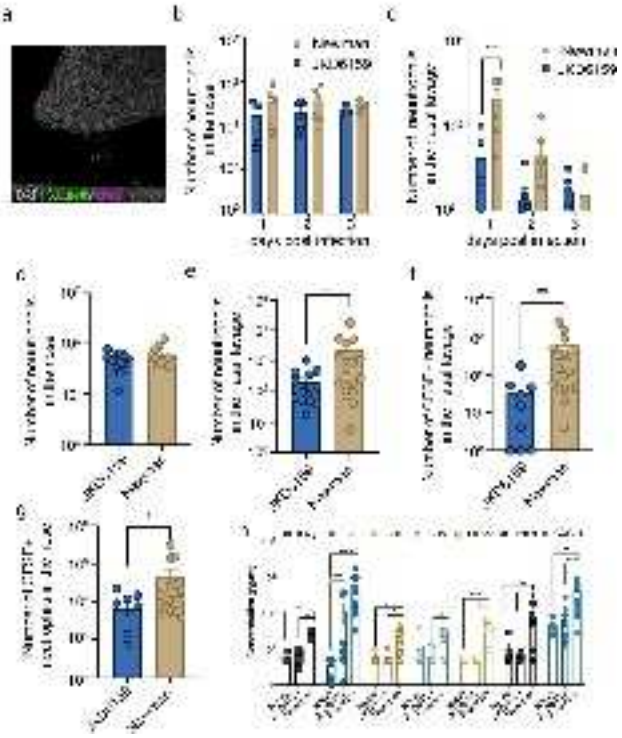

imcb_12343_f3.tif

This article is protected by copyright. All rights reserved

Author Manuscript

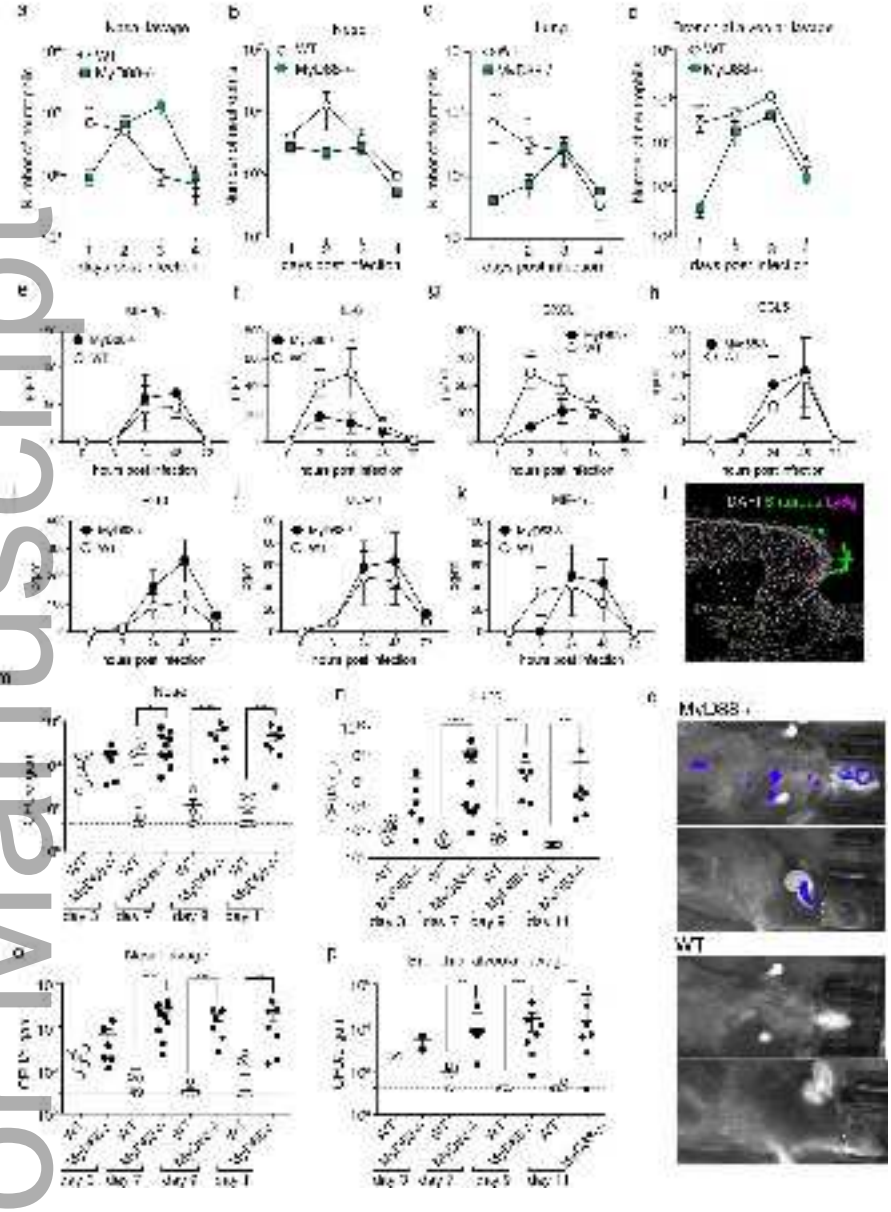

imcb_12343_f4.tif

This article is protected by copyright. All rights reserved

Figure 5

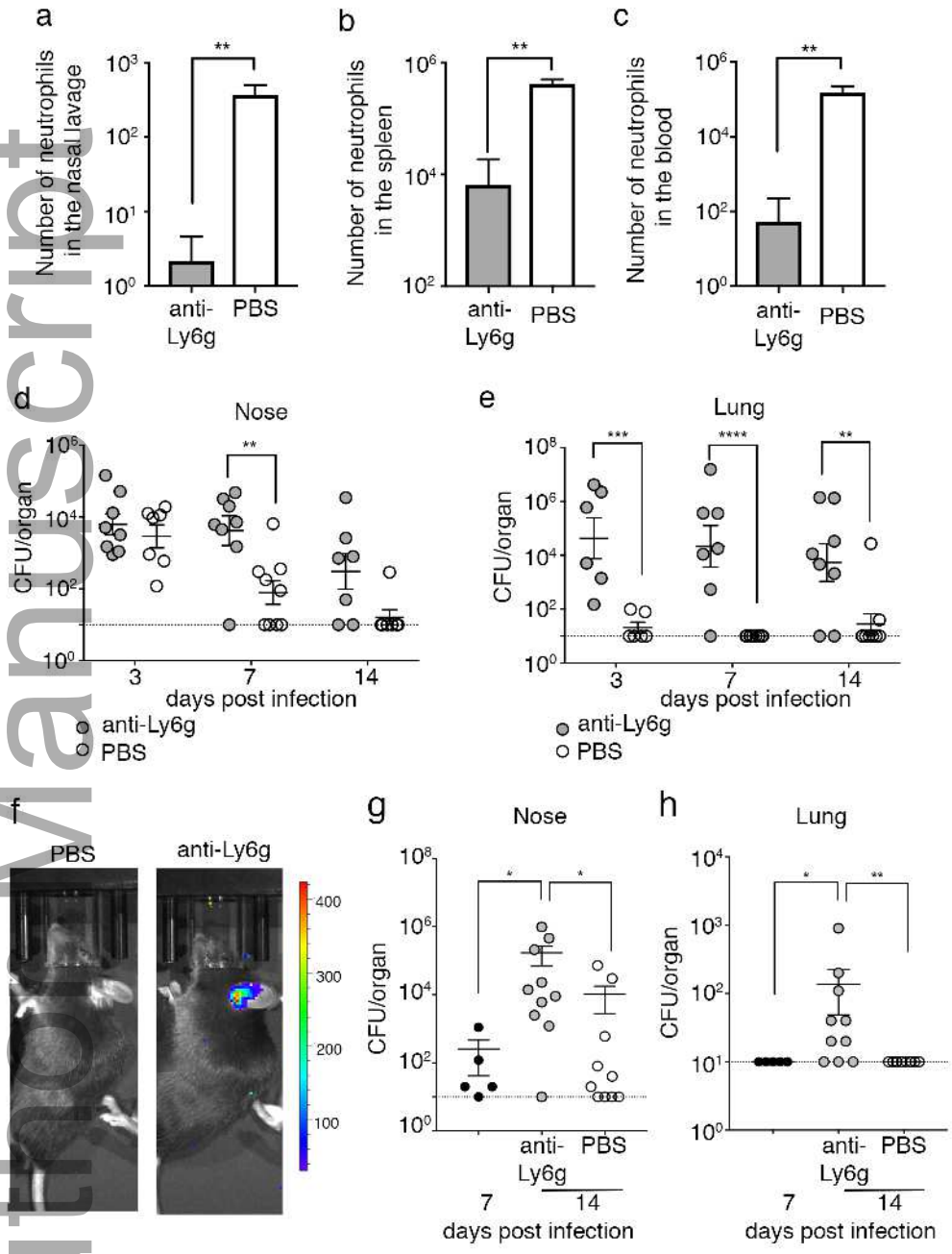


imcb_12343_f5.tif

Author Manuscript

This article is protected by copyright. All rights reserved

Figure 6

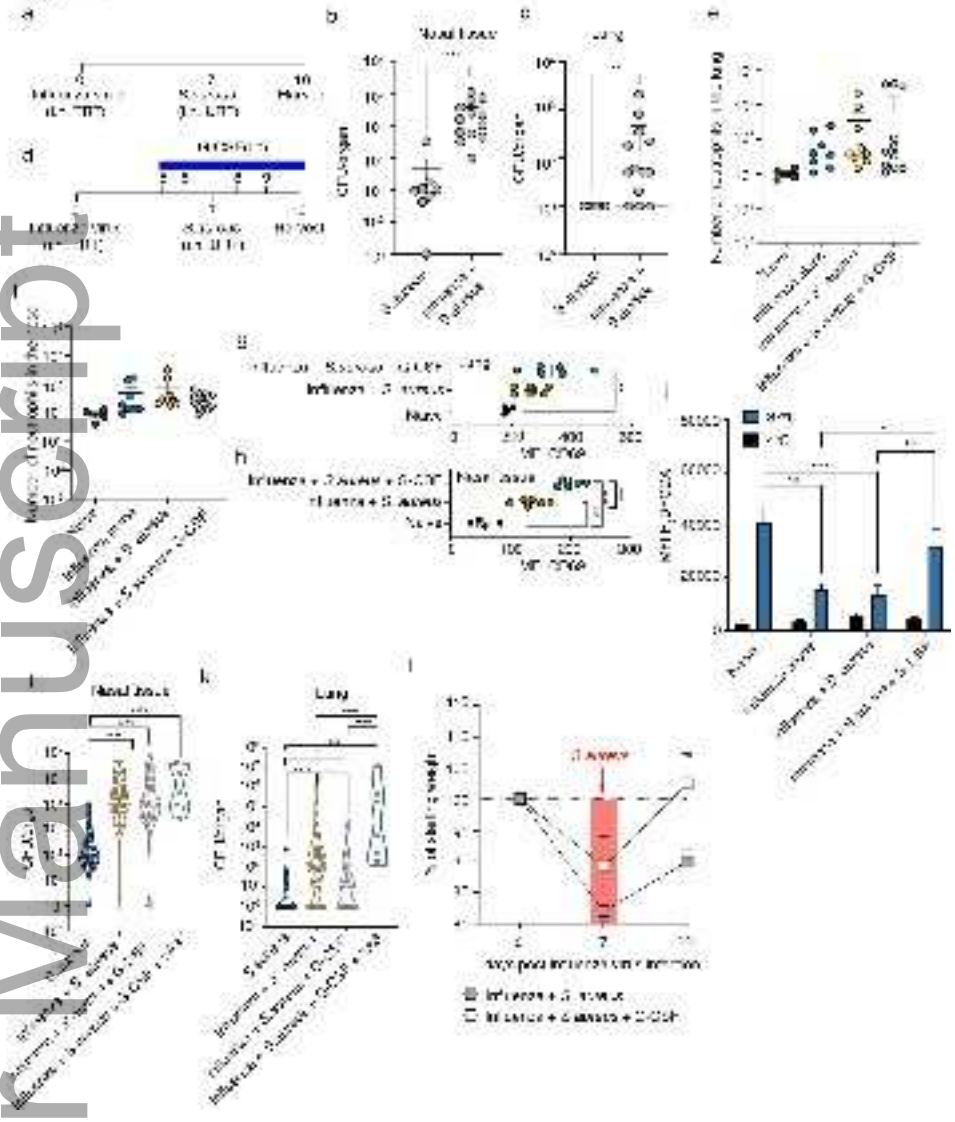

imcb_12343_f6.tif

Author Manuscript

This article is protected by copyright. All rights reserved